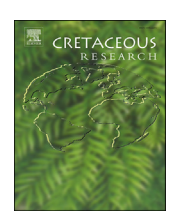
ELSEVIER

Contents lists available at ScienceDirect

Cretaceous Research

journal homepage: www.elsevier.com/locate/CretRes



Cretaceous fossil gecko hand reveals a strikingly *modern* scansorial morphology: Qualitative and biometric analysis of an amber-preserved lizard hand



Gabriela Fontanarrosa ^a, Juan D. Daza ^b, Virginia Abdala ^{a, c, *}

- ^a Instituto de Biodiversidad Neotropical, CONICET, Facultad de Ciencias Naturales e Instituto Miguel Lillo, Universidad Nacional de Tucumán, Argentina
- ^b Department of Biological Sciences, Sam Houston State University, 1900 Avenue I, Lee Drain Building Suite 300, Huntsville, TX 77341, USA
- ^c Cátedra de Biología General, Facultad de Ciencias Naturales, Universidad Nacional de Tucumán, Argentina

ARTICLE INFO

Article history: Received 16 May 2017 Received in revised form 15 September 2017 Accepted in revised form 2 November 2017 Available online 14 November 2017

Keywords: Squamata paleobiology Paraphalanges Hand evolution

ABSTRACT

Gekkota (geckos and pygopodids) is a clade thought to have originated in the Early Cretaceous and that today exhibits one of the most remarkable scansorial capabilities among lizards. Little information is available regarding the origin of scansoriality, which subsequently became widespread and diverse in terms of ecomorphology in this clade. An undescribed amber fossil (MCZ R-190835) from mid-Cretaceous outcrops of the north of Myanmar dated at 99 Ma, previously assigned to stem Gekkota, preserves carpal, metacarpal and phalangeal bones, as well as supplementary climbing structures, such as adhesive pads and paraphalangeal elements. This fossil documents the presence of highly specialized adaptive structures. Here, we analyze in detail the manus of the putative stem Gekkota. We use morphological comparisons in the context of extant squamates, to produce a detailed descriptive analysis and a linear discriminant analysis (LDA) based on 32 skeletal variables of the manus. The comparative sample includes members of 15 extant squamate families (Agamidae, Dactyloidae, Iguanidae, Leiosauridae, Liolaemidae, Polychrotidae, Tropiduridae, Diplodactylidae, Eublepharidae, Gekkonidae, Phyllodactylidae, Sphaerodactylidae, Gymnophthalmidae, Teiidae, and Scincidae). Although the fossil manus is qualitatively more similar to that of members of Gekkota, the LDA analysis places it in a morphozone shared by Gekkota and Scincomorpha. This result is particularly interesting, given that despite the presence of paraphalangeal structures had only been reported in extant geckos of the families Gekkonidae and Phyllodactylidae, the usage of an adhesive subdigital system to climb originated independently in Gekkota, Scincidae, and Dactyloidae.

© 2017 Elsevier Ltd. All rights reserved.

1. Introduction

Extinct faunas are intriguing, probably because they document bits of information from the past. Among fossil faunas, those represented by amber inclusions are among the best preserved; amber fossils offer superb detail and three-dimensional preservation (Grimaldi, 1996; Ross, 2010). Recently, Daza et al. (2016) reported an amber assemblage of mid-Cretaceous lizards from Myanmar, with such extraordinary preservation that it allowed confidently allocate them to higher taxonomic ranks. Among these amber fossils, a manus preliminarily assigned to the stem Gekkota was found (MCZ R—190835). This hand preserves all the phalangeal,

* Corresponding author.

E-mail address: virginia@webmail.unt.edu.ar (V. Abdala).

metacarpal, and carpal elements, together with the distal epiphyses of the radius and ulna. Additionally, we identified several pairs of putative paraphalangeal elements.

The interpretation of the fossil record of vertebrates is biased

The interpretation of the fossil record of vertebrates is biased towards cranial elements, and postcranial remains are usually underestimated due to taphonomic and sampling problems, typically being more difficult to identify when isolated and often providing fewer diagnostic features than the skull (Rubidge, 2013). The amber-preserved hand of MCZ R—190835 represents an exception that allows us to extrapolate morphological aspects and apply them to the ecology associated with limb structure. Gekkota is a very diverse and widespread clade, containing more than 1700 extant species (Gamble et al., 2012; Uetz et al., 2017). Because the group remains poorly represented by pre-Quaternary fossils (Estes, 1983; Augé, 2005), the past ecological history of geckos has largely

been reconstructed from character analyses based on features of extant members of the clade. However, certain new fossils from the Mesozoic have been classified as gekkotans or stem-gekkotans, including material from the Lower to Upper Cretaceous of Myanmar, Mongolia and West Siberia (Daza et al., 2014). Among those fossils, *Cretaceogekko burmae* is particularly relevant, because it provides evidence of the early presence of scansorial abilities in the group. This fossil exhibits specialized subdigital structures of modern appearance (Arnold and Poinar, 2008), although this statement is based exclusively on external features, since no skeletal features have been found (T. Hagey, personal communication). MCZ R-190835 reveals new important aspects of the evolution of scansoriality in geckos of the mid-Cretaceous from an internal anatomy perspective.

Scansoriality through adhesive toepads has evolved multiple times among squamates, including Dactyloidae, Scincidae (Prasinohaema spp.), and most notably, geckos, among which these structures were estimated to have appeared at least 11 times (Gamble et al., 2012; Higham et al., 2015). Throughout this manuscript, we use the term scansorial to refer to all the lizards that are capable of clinging on vertical surfaces by means of scansors or toepads. One common idea about the underlying mechanism of toepad adhesion indicates that millions of setae interact with the substrate through van der Waals forces and friction (Cartmill, 1985; Russell, 2002), although a recent proposal suggests that gecko toepads develop electrostatic interactions with the substrate (Izadi et al., 2014). The precise control of the kinematics of the setal attachment and detachment is performed via a complex musculoskeletal network (Russell and Bauer, 1988; Russell, 2002). This network often includes skeletal structures adjacent to the medial and lateral aspects of some of the interphalangeal joints, such as the paraphalangeal elements, which have been exclusively reported in some pad-bearing gekkonid and phyllodactylid lizards (Romer, 1956; Russell and Bauer, 1988; Gamble et al., 2012; Higham et al., 2015). These elements seem to play a role in the placement of toepads onto the substrate, and have also been perceived as associated with digging, climbing and grasping (Russell and Bauer, 1988). Finally, not all the pad bearing geckos exhibit paraphalangeal elements (Russell and Bauer, 1988; Gamble et al., 2012). In the present work, we analyze in detail the anatomy of MCZ R-190835, and evaluate its qualitative and quantitative similarities with scansorial and non-scansorial squamates.

2. Materials and methods

2.1. Data acquisition

The specimen MCZ R-190835 was imaged using highresolution 3D x-ray computed tomography. A GE phoenix v|tome|x s240 system, with a molybdenum target and modification of the current and voltage to maximize the range of densities recorded was used to collect the data. 3D rendering and segmentation were performed using VGStudio MAX version 2.2 (Volume Graphics GmbH) and Avizo Lite 9.0.0 (Visualization Sciences Group). A rotation movie with the 3D volume-rendering was used as a data source regarding bones of the manus, and the details were inspected directly on Avizo Lite 9.0.0. The general anatomy of the fossil manus was based on digital images. A brief survey of the morphological diversity of the paraphalangeal features in geckos, based on our specimen sample and published descriptions were included. A brief survey of the variation of the ungual phalanx morphology among scincomorphs and gekkotans, in order to compare the fossil hand with extant forms, was also performed.

In addition, a morphometric data set with 51 variable attributes of the hand using 428 specimens was assembled (Supplementary

Data). The sample consists of 69 genera representing 16 squamate families (Gekkota 5, Iguania 7, and Scincomorpha 4; Estes et al., 1988; Conrad, 2008; Gauthier et al., 2012). The sample was assembled to fulfill two main objectives: (1) maximizing the morphological range of variation, and (2) maximizing phylogenetic representation (including only squamate lineages with fully developed limbs). Measurements were taken from radiographed specimens (140 specimens) and from digital photographs from cleared and double stained skeletons previously prepared following Wassersurg (1976) protocol (288 specimens). Photographs were taken with a stereo dissecting microscope (Nikon, SMZ-10, Nikon Corp., Tokyo, Japan). The attributes considered were length and width of each bone of the manus. Measurements from ungual phalanx were disregarded because the presence of claw sheath obscures its boundaries. Measurements were processed using the image processing package Fiji (Schindelin et al., 2012). Each specimen was measured three times and the arithmetic mean was used. In order to determine the number of decimals to be included, a coefficient of variation based on a subset of specimens was calculated, and three decimals were included because they captured information in a relevant resolution. Even though we combined measurements from radiographs and cleared and stained specimens that might not be entirely conveying the same information, the power of a bigger data set justifies this approach.

2.2. Data analyses

To determine the morphological similarities of the fossil hand with taxa from our sample, we performed a Linear Discriminant Analysis (LDA). This method is used to find a linear combination of variables (predictors) that maximizes the separation between two or more classes within the data. At the same time, it minimizes the variation within each class of data. The method requires the assignment of *a priori* membership of a sample to a given class. The set of samples established *a priori* (with a known class) is used as a training set to construct the linear combination of variables (discriminant function) that best explains the differences between classes. In the current study we used taxonomic grouping as the class criterion.

To determine the morphometric similarities of the fossil specimen, the method incorporates the measurements of that particular specimen into the (already built) discriminant function to assign it to one of the given classes. To validate the built discriminant function, we retained three specimens of a known class, without providing that information to the software, and inserted them as points into the built morphospace. The validation sample consisted of: one specimen of Gekko hokouensis (USNM 219634), one specimen of Cnemidophorus longicaudus (VA1.4), and one specimen of Anolis maculiventris (MUI 4388). Since the validation samples fit in the assigned class, we considered the discriminant functions to be rigorous in their predictive ability. To improve the validation process, specimens that were retained included (whenever possible) both members and non-members of a taxonomic class. For example, in the LDA performed for the gekkotan data set, we used both gekkotan (internal) and non-gekkotan (external) validation specimens.

Initially, the classes in our data corresponded to three main clades within Squamata (Gekkota, Scincomorpha, and Iguania). In a second step, and based on the outcome of the first step, a LDA including only the classes Gekkota and Scincomorpha was performed. In a third step, considering that our anatomical analysis showed putative paraphalanges in a digit of the amber hand, and that such structures have been described only for extant gekkotans, a subtler analysis of the Gekkota, including five families as classes (Gekkonidae, Sphaerodactylidae, Diplodactylidae, Eublepharidae

and Phyllodactylidae) was performed. For all steps we superimposed the fossil specimen onto each resulting morphospace. In the three mentioned steps, the original variables used to create the linear discriminant functions were derived from the metacarpal and digital regions, but carpal variables were excluded. This set of original variables was selected because, in the fossil hand, the boundaries of the bones of the carpal region are mostly indistinguishable (see Results). Regardless, an alternative LDA based on gekkotan data using variables derived from the carpal region (Supplementary Data) was developed, in order to ascertain the relevance of such variables for the manual morphological identification within Gekkota. However, for this purpose, we were unable to superimpose the fossil specimen because the LDA cannot accommodate missing data. The output of the LDAs is presented as a scatter plot of one or two dimensions, together with a score table of the numerical values of each specimen resulting from the outcome of the linear discriminant function. The scores locate the position of each specimen within the morphospace, while the score table allows us to assess the similarities of the fossilized specimen in relation to each specimen in the table.

All the statistical analyses were performed in R statistical language and environment (R Development Core Team, 2011).

2.3. MCZ R-190835 provenance and repository

The amber-preserved-hand derives from mid-Cretaceous outcrops in Kachin Province, northern Myanmar, approximately 100 km west from Myitkyina City. Amber from Burma was radiometrically dated at 99 Ma using U–Pb isotopes (Shi et al., 2012). This result places the deposit age close to the Aptian-Cenomanian boundary. For further information on the age estimation see Shi et al. (2012). MCZ R–190835 is housed in Museum of Comparative Zoology, Harvard University, Cambridge, USA.

2.4. Extant specimens repositories

The specimens of extant taxa considered for the morphometric matrix are hosted in the following institutions: Fundación Miguel Lillo, Tucumán, Argentina (FML and SAUR); Universidad Nacional de Salta, Salta, Argentina (MCN); Universidad Nacional del Noroeste, Corrientes, Argentina (UNNEC); Museo de La Plata, La Plata, Buenos Aires, Argentina (MLP); Universidad Industrial de Santander, Bucaramanga, (UIS); Pontificia Universidad Javeriana, Bogotá, Colombia (MUJ); Museo de Herpetología, Universidad de Antioquia, Colombia (MHUA); Universidad Nacional de Colombia, Bogotá, Colombia (ICN); United States National Museum, Washington, U.S.A. (USNM); Field Museum of Natural History, Chicago, U.S.A. (FMNH); Virginia Abdala colection, Instituto de Biodiversidad Neotropical, Tucumán, Argentina (VA).

3. Results

3.1. Anatomical description (Figs. 1 and 2)

Specimen MCZ R—190835 corresponds to a left manus that preserves all the phalangeal, metacarpal, and carpal elements, articulated with the distal forelimb region. The presence of skin impressions allowed to confirm the correlation of the position of the toepads with the phalanges (Daza et al., 2016; Fig. 1). The carpal elements exhibit no clear edges (Fig. 2). In the carpal region there are two ambiguous structures: 1) The putative pisiform (Daza et al., 2016) that contacts the ulnare is situated in a more ventral plane when compared to the other carpals, and is proportionally larger than that of extant squamates. This piece could therefore alternatively be interpreted as the distal epiphysis of the ulna; 2) The

interpreted radial process is a ventral protuberance of the radiale, ventrally coplanar with the putative pisiform (Fontanarrosa and Abdala, 2014); alternatively, the structure could be the first distal carpal, as identified by Daza et al. (2016). Between the ventral projection of the radial process and the pisiform there is a narrow channel lying at the base of the hand. The remaining carpal structures cannot be accurately described, although they seem to be complete. Metacarpals I and V are sub-equal in length and are the shortest metapodials; metacarpals II, III, and IV are sub-equal in length and are 1.5 times longer than I and V. The distal epiphyses of metacarpals II, III and IV are slightly wider than the proximal ones. The phalangeal formula is 2-3-4-5-3 (Fig. 2). The first phalanges of each digit are sub-equal in length. The distal head of the basal phalanx of the first digit is narrower than the proximal one. In the second, third and fourth digits, the distal head of the basal phalanges is semi-spherical and wider than the proximal head. In the basal phalanx of the fifth digit, both extremities are sub-equal in width. In each digit, penultimate phalanges are the longest ones, each of which exhibits a slightly concave ventral surface. The ungual phalanges are short in relation to the overall digit length and are tall at their proximal end. The first and fifth ungual phalanges appear to be of similar size (approximately 1/3 of the length of their respective penultimate phalanges), and both are shorter than the unguals of the second, third and fourth digits. The fourth digit is a relatively tall structure, and bears the largest ungual phalanx, which is also the best preserved of the unguals, although it lacks of a claw sheath (Table 1). The unguals of the first, second and third digits apparently preserves the claw sheath, but it seems to be deformed. The ungual phalanx of the fifth digit seems to lack of a claw sheath and is also distorted. Each ungual phalanx exhibits a pronounced curvature in the ventral claw arc, interrupted by a sharp ventral inflection (Tinius and Russell, 2017). Aligned with this ventral protrusion, the dorsal aspect of the ungual contains a concavity bordered by two peaks (Table 1).

The third and fourth digits are equal in length, and are the longest. The second and fifth digits are subequal in length, shorter than the third and fourth digits, but longer than the first digit.

The digital divergence, measured as the angle formed between the first and the fifth metacarpals, is around 52°.

The metacarpophalangeal joints seem to be of ellipsoidal type (Kümmell and Frey, 2012). The interphalangeal joints appear to be hinge joints (Neumann, 2010; Kümmell and Frey, 2012), suggested by the pronounced symmetrical bicondyle situated in both sides respect a groove as seen in the distal end of each phalanx in their dorsal view. The ventral aspect of the proximal extreme is proximally extended beneath the distal head of the consecutive proximal phalanx (see pre-ungual phalanx of digit IV in Fig. 3A, and Russell and Bauer, 2008). Small circular plate structures with either external, medial, or lateral concave surfaces are present close to some of the digits (Fig. 3A). In dorsal view, towards the lateral side of the metacarpophalangeal joint of the first digit, there is only one of such structures. In the medial side of the metacarpophalangeal joint of the fifth digit, there is a single structure. In the middle of the distal epiphyses of the fourth metacarpal there is one of these structures with another one proximate to the latter. On the medial and lateral sides of the distal end of the first phalanx of the fourth digit, there is a pair of discoidal structures, with another pair at the metacarpophalangeal joint of the same digit (Fig. 3B). One of these structures is also present between the third and fourth phalanx of digit IV. In ventral view, there are four of these structures, scattered along the second phalanx of the second digit. Another of these structures is placed on the ventromedial side of the metacarpophalangeal joint of the same digit. The above-mentioned structures are topologically equivalent to the paraphalangeal elements of certain extant geckos (Fig. 3C and Table 2).

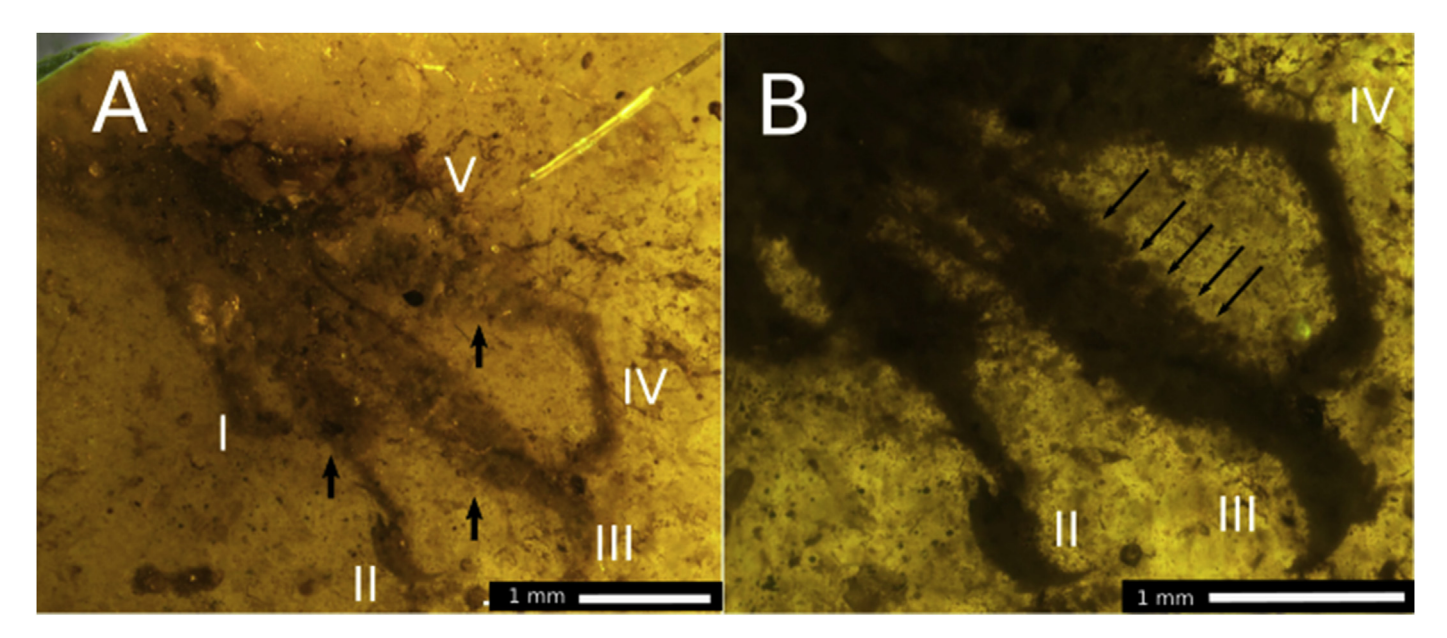


Fig. 1. External morphology of the specimen MCZ R-190835, ventral view. (A) The skin impressions of the adhesive subdigital pads composed by laterally expanded scales or lamellae are showed with arrows. Pads are clearly noted in digits II, III and IV. (B) Close up of digits II, III and IV. Arrows are indicating the boundaries between successive lamellae of digit III. Photographs courtesy of David Grimaldi.

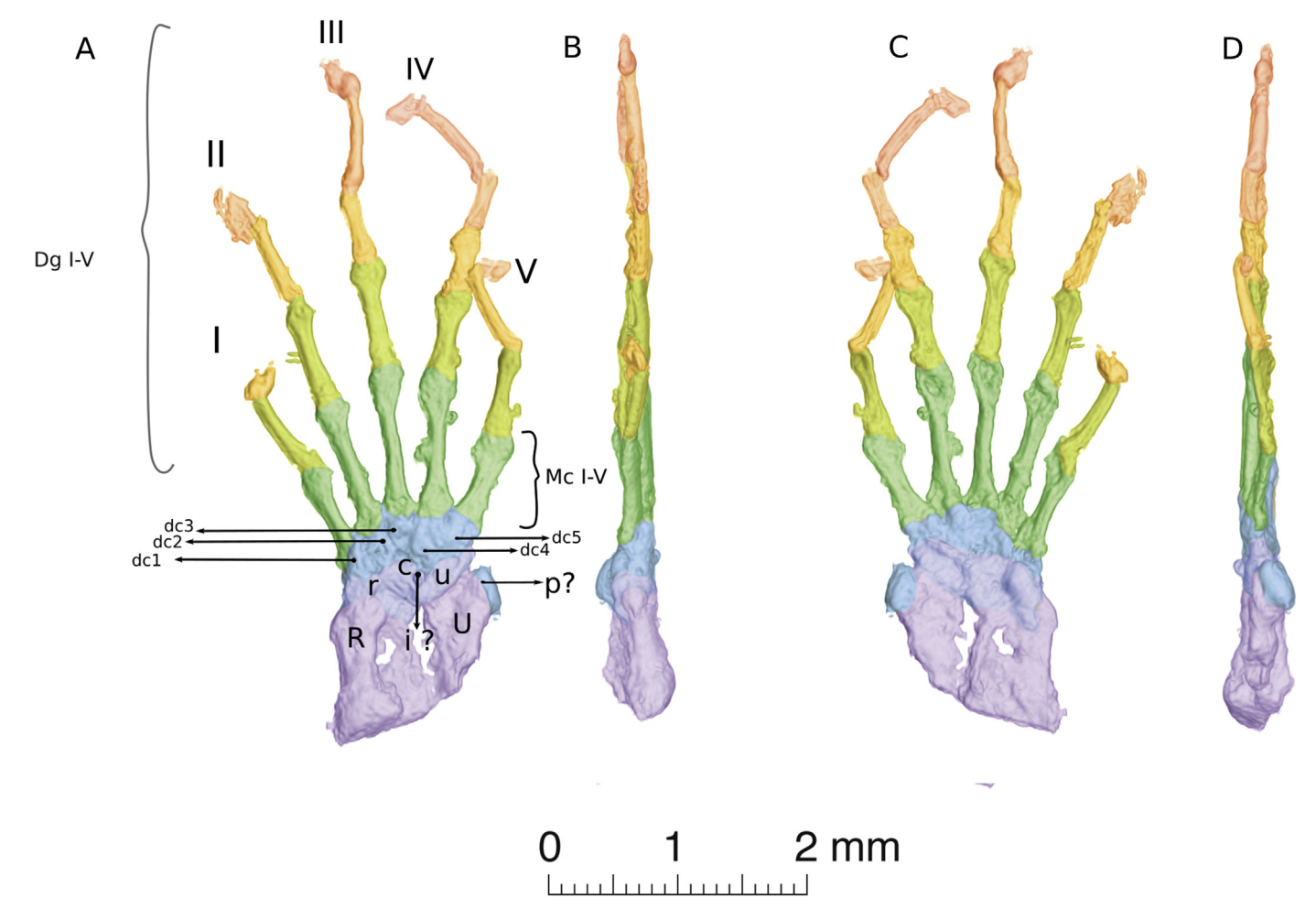


Fig. 2. MCZ R-190835 μCT. (A) dorsal view with the identity of the elements indicated. (B) μCT, mesial view (C) μCT, ventral view. (D) μCT, lateral view. R: radius; U: ulna; r: radiale; u: ulnare; c: centrale; dc1-5: distal carpalia 1-5; Dg: digits I-V, Mc I-V: metacarpals I-V; p?: pisiform?; i?: intermedium?.

Table 1Ungual phalanges of some squamates (drawings not to scale). V. inflection = Ventral inflection; D. concavity = Dorsal concavity; Y = present; N = absent.

Species	Group	Shape	Downward inflection (Y/N)	Dorsal concavity (Y/N)
Hemidactylus mabouia	Gekkota		Y	N
Homonota fasciata	Gekkota		N	N
Phyllopezus pollicaris	Gekkota		Υ	Y
Hoplodactylus duvauceli	Gekkota		Y	Y
Emoia atrocostata	Scincomorpha		Y	Y
Emoia pallidiceps	Scincomorpha		Υ	N
Mabuya mabouya	Scincomorpha		Υ	N
Mochlus sundevallii	Scincomorpha		Y	N
lguana iguana	Iguania		Υ	Y
Anolis tolimensis	Iguania		Y	Y?
Polychrus acutirostris	Iguania		Y	N
Phymaturus palluma	Iguania		Y	N
Tropidurus torquatus	lguania		Y	N
Fossilized specimen MCZ R-190835	Stem-Gekkota		Y	Y

3.2. Morphological diversity of the ungual phalanx of extant squamates (Table 1)

The downward pointed curvature of the ungual observed in MCZ R-190835 is also present in several other squamate genera. The dorsal concavity observed in MCZ R-190835 is less common, but is present in certain iguanians and scincomorphs (Table 2).

3.3. Morphological diversity of the paraphalangeal elements in extant members of the Gekkonidae and Phyllodactylidae (Table 2)

Sixteen genera of gekkotans are known to exhibit paraphalangeal elements, all of them belonging to the Gekkonidae or Phyllodactylidae families. We discovered these elements in the phyllodactylid genus *Homonota*, in which they are relatively small

and discoidal. The paraphalanges in *Homonota* are located laterally to the distal epiphyses of metacarpals two to five. The medial and lateral paraphalangeal pair is frequently asymmetrical in size. Paraphalanges stain red in cleared-and-double-stained adult specimens, indicating the presence of calcium in the structure (Wassersurg, 1976), and they are embedded in the extensive lateral digital tendons. Paraphalanges were found in all the examined *Homonota fasciata* specimen (UNNEC 07717, UNNEC 09158, SAUR 00794-2, FML 01751-2, FML 01571-2). Paraphalanges appear to be absent in the other *Homonota* species examined: *H. darwinii*, *H. whitii* and *H. uruguayensis*.

3.4. LDA. First step: Exploration of the squamate dataset (Fig. 4)

The three validations performed for the squamate LDA corroborated the accuracy of the analyses. The first linear discriminant

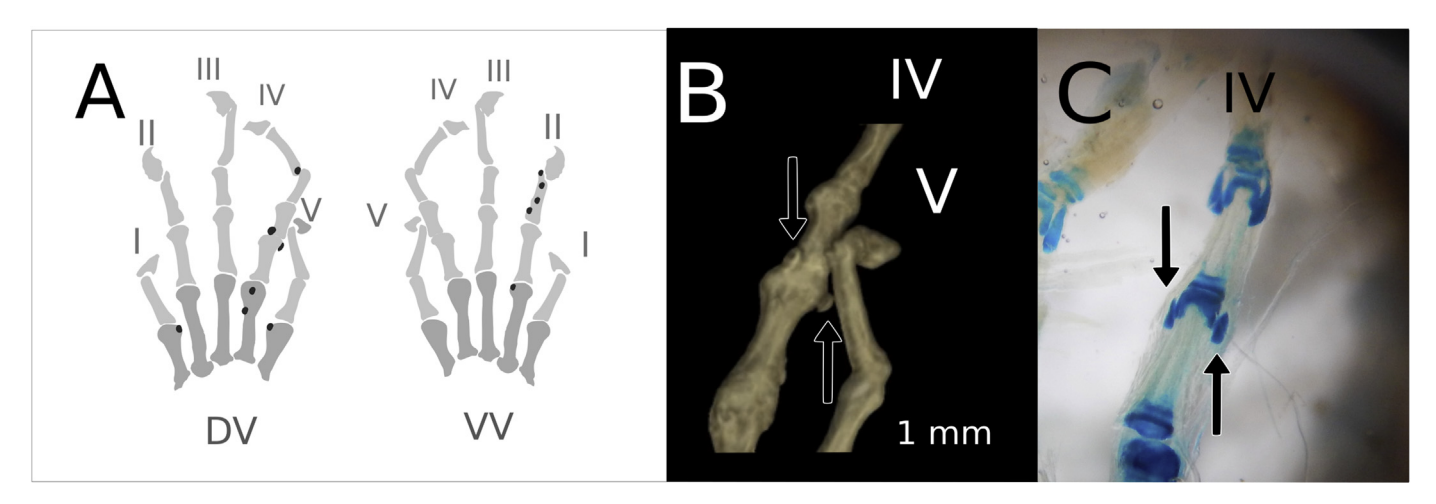


Fig. 3. Metacarpals and digits schematic of MCZ R-190835 in dorsal and ventral view. (A) Distribution of the circular plates structures is shown (black). Metacarpals are shown in dark gray and digits in light gray. Seven structures are described in dorsal view and five in ventral view. (B) Enlarged dorsal view of digits IV and V of the MCZ R-190835 hand showing a pair of circular elements. The two structures are located mesial and lateral to the interphalangeal joint between the first and second phalanges of the fourth digit, with the mesial element slightly displaced distally. The putative paraphalanges are discoidal and relatively small. (C) Cleared and stained left hand of *Hemidactylus mabouia* (FML 2142) in dorsal view showing a distal pair of paraphalangeal elements and a more proximal pair of discoidal paraphalangeal elements. The latter pair is located to the medial and lateral side of the interphalangeal joint between the first and second phalanges of the fourth digit (i.e., similar to where the putative paraphalangeal elements are present in the fossil hand). Note also that the proximal pair of paraphalanges of *H. mabouia* are morphologically similar to the pair of structures shown in A. Abbreviations: **DV**: Dorsal View; **VV**: Ventral View.

function (LD1) separates Gekkota (GK) from Scincomorpha (SC) + Iguania (IG). LD1 accounts for 90% of the total variability that separates specimens of the taxonomic groups (Fig. 3). The gekkotan taxa cluster is in the negative zone of LD1. LD2 separates iguanian and scincomorph morphozones. There is a slight marginal overlap of taxonomic morphospaces. The fossil specimen lies within the scincomorph morphozone (Fig. 3A). Nevertheless, this portion of the morphozone, where the fossil hand is located, is also shared by members from all the three main categories.

Table 3 shows the values of the specimens in the bi-dimensional space circumscribing the LDA (scores). Specimens from *Ameiva ameiva* (Scincomorpha: Teiidae) and *Polychrus acutirostris* (Iguania: Polychrotidae) exhibit the most similar proportions to those of the fossil specimen, considering both axes. Only specimens with scores close to the fossil's LD1 are shown. Considering only LD1, *Emoia atrocostata*, *Cnemidophorus longicaudus*, *Ameiva ameiva*, *Pseudogonatodes peruvianus*, and *Saurodactylus mauritanicus* are close neighbors. Thus, the fossil hand exhibits similar proportions to scincomorphs, and is also adjacent to certain miniaturized species of geckos (e.g. *Pseudogonatodes peruvianus* and *Saurodactylus mauritanicus*).

3.5. LDA. Second step: Exploration within the Gekkota + Scincomorpha dataset (Fig. 5)

In this analysis a one-dimensional LDA was performed. The fossil hand has been predicted to be placed within the scincomorph morphozone. The morphozones of Gekkota and Scincomorpha are well defined, although they share an area around the 0 value of the axis. The fossil hand was plotted within a region of the scincomorph morphozone that shows a slight overlap with the boundary of the Gekkota group. Comparing the scores along LD1 (Table 4), it was found that those for the scincomorphs *Mochlus sundevallii*, *Marmorosphax tricolor*, *Mabuya mabouya* and *Emoia longicauda* are the closest to that of the fossilized specimen MCZ R—190835. *Cyrtodactylus agusanensis* is the closest gekkotan species to the fossil specimen in this analysis.

3.6. LDA. Third step: Exploration within the Gekkota dataset (Fig. 6)

Considering metacarpal and digital variables (Fig. 6A), the morphozones of the gekkotan families show a minor overlap. The fossil specimen projects into the area occupied by Phyllodactylidae and Eublepharidae. Considering carpal, metacarpal and digital variables (Fig. 6B) the analysis separates five clusters that correspond to Diplodactylidae, Eublepharidae, Phyllodactylidae, Sphaerodactylidae and Gekkonidae.

3.7. Comparison of hand morphology

We compare the overall morphology of the fossil hand to that of certain pad-bearing geckos (Fig. 7A) and scincomorphs (Fig. 7B) in order to correlate their shape with the results from the LDA analyses. The metacarpal proportions of the fossil hand are similar to those of *Mabuya* sp. or *Aristelliger* sp.; the digit divergence angle of the fossil hand (of 52°), is more similar to that of the scincomorph specimens than to that of the gekkotans. Taking into account the length of the digits, the fossil hand is more similar to that of *Mabuya* sp.

4. Discussion

The qualitative analysis of the anatomical traits and the biometrical characteristics of the fossil hand produces contrasting results. Morphological data indicates that the specimen could be allocated within Gekkota. The fossil hand shows remains of toepads and paraphalangeal elements followed by a slender phalanx and expanded distal extremes of certain phalanges, a combination of characteristics present in extant geckos such as *Thecadactylus* sp. (Gamble et al., 2012) and *Gehyra mutilata* (Russell, 2002). Specifically, in the fossilized hand MCZ R—190835, the distal extreme of the basal phalanx of digit I is narrower than its proximal epiphysis. In digits II to V, the proximal phalanges have wider distal ends than the following distal phalanges. This pattern of differential morphology of the basal phalanges is also evident in

Table 2Examples of gekkotan genera with paraphalangeal elements, and comparison with MCZ R—190835. The digits are shown as fully extended. Skeletal elements of the fourth digit of each genus in light gray. Paraphalangeal elements in dark gray.

Genus	Configuration	Adhesive toe pads (Yes/No)	References
Gekkonidae			
Gehyra		Y Manus	Wellborn (1933), Stephenson (1960), Gamble et al. (2012)
Uroplatus		Y Pes	Wellborn (1933), Russell and Bauer (1988), Gamble et al. (2012)
Hemidactylus		Y Manus	Wellborn (1933), Stephenson (1960), this work
Lygodactylus		Y Manus	Wellborn (1933), Gamble et al. (2012)
Hemiphyllodactylus		Y Pes	Kluge (1968), Gamble et al. (2012)
Perochirus		Y Pes	Russell and Bauer (1988), Gamble et al. (2012)
Phyllodactylidae Homopholis		Y Pes	Russell and Bauer (1988), Gamble et al. (2012)
Calodactylodes		Y Pes	Russell and Bauer (1988), Gamble et al. (2012)
Pachydactylus	Park,	Y/N Pes	Haacke (1976), Russell and Bauer (1988), this work
Blaesodactylus		Y Pes	Gamble et al. (2012)
Geckolepis		Y Pes	Gamble et al. (2012)
Afroedura		Y	Gamble et al. (2012)
Phyllopezus		Y Pes	Russell and Bauer (1988), Gamble et al. (2012)
Thecadactylus		Y Manus	Russell and Bauer (1988), Gamble et al. (2012), this work
Homonota		N Manus	This work
Stem Gekkota Fossil hand		Y Manus	Daza et al. (2016), this work

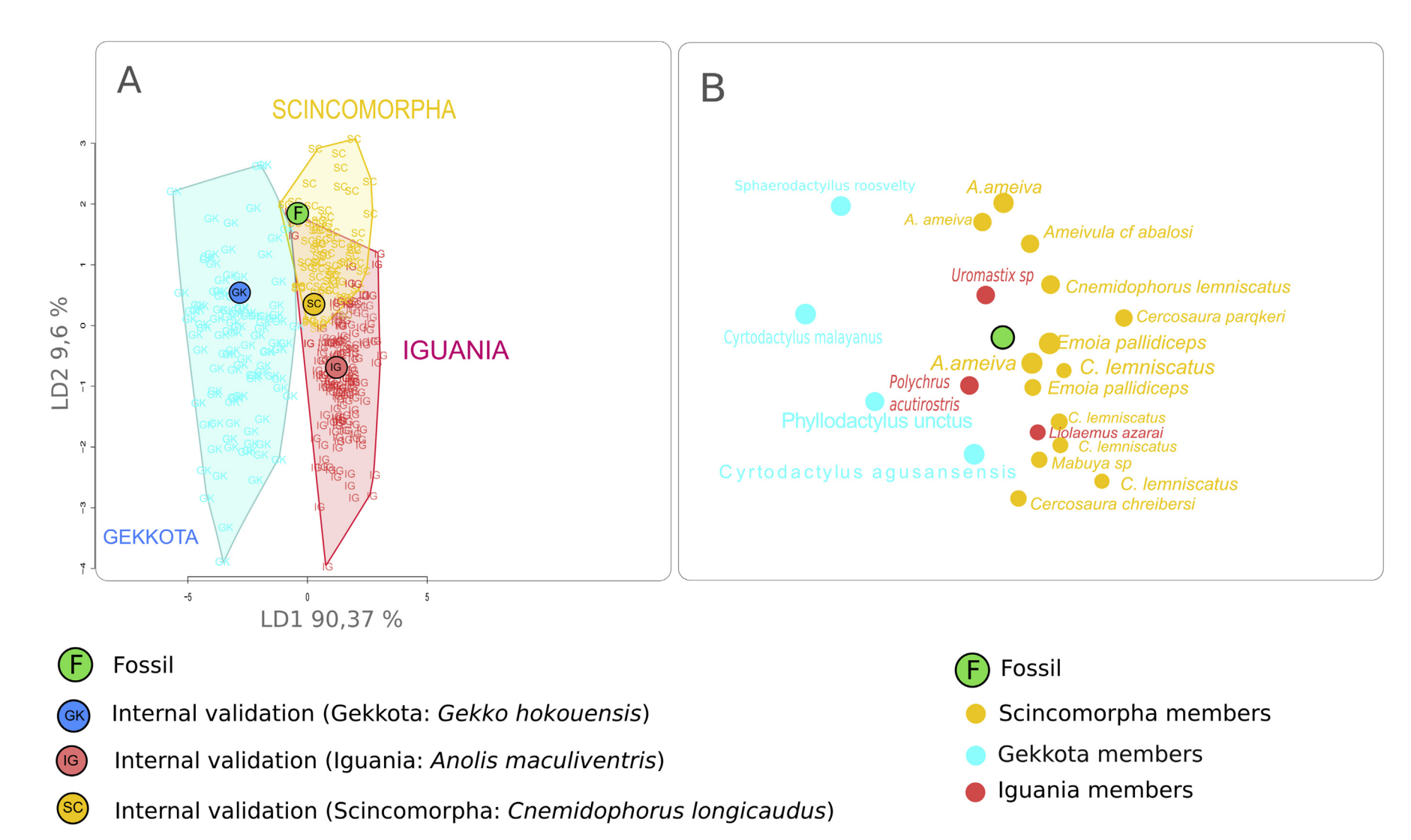


Fig. 4. Fossil hand projected onto the squamate LDA. (A) The fossil lies at the boundary of the scincomorph morphozone. A validation dot is correctly assigned to each major clade. The polygons enclose specimens of each class considered. (B) Detail of the fossil hand and its closest species within the morphospace. The closest species are *Polychrus acutirostris* (Dactyloidae), *Emoia pallidiceps* (Scincidae), *Ameiva ameiva* (Teiidae), and *Uromastyx* sp. (Agamidae). The colored dots indicate taxa: Gekkota, Iguania and Scincomorpha.

Table 3LDA Scores (First Step). The specimens are ordered by increasing LD1 score. The scores represent the position of each specimen in the morphospace defined by the analysis. The analysis is based upon three categories for which two linear discriminant functions (LD1 and LD2) were obtained. LD. = Collection identification. The score of the fossilized specimen MCZ R—190835 is included. The closest values to the fossil hand are highlighted in bold.

Species	Group	Specimen number	Ordered scores along LD1	Ordered scores along LD2
Ameiva ameiva	Scincomorpha	ICN 4668	-0.022	-0.179
Mabuya mabouya	Scincomorpha	UIS 0355 RC 053	-0.090	1.006
Cnemidophorus longicaudus	Scincomorpha	VA 003/4	-0.154	-0.157
Emoia atrocostata	Scincomorpha	USNM 195779	-0.448	-1.711
MCZ R-190835	Stem Gekkota	MCZ R-190835	-0.491	1.781
Pseudogonatodes peruvianus	Gekkota	USNM 343190	-0.537	-2.132
Ameiva ameiva	Scincomorpha	ICN 4753	-0.619	-1.833
Ameiva ameiva	Scincomorpha	UNNEC 01390	-0.630	1.949
Polychrus acutirostris	Iguania	UNNEC 04366	-0.675	1.433
Saurodactylus mauritanicus	Gekkota	USNM 217454	-0.846	-0.035
Uromastyx sp.	Scincomorpha	MCN 4627	-0.865	2.193
Cyrtodactylus agusanensis	Gekkota	USNM 318433	-0.980	-1.01

some extant diplodactylid geckos, such as Dactylocnemis pacificus. The second phalanx of the fourth digit also shows an expanded distal end, followed by a slender third phalanx. It could be inferred that the expanded extreme might be functionally associated with the paraphalangeal elements. Although pads are not exclusive of extant gekkotans, expanded phalangeal ends apparently are (Russell and Bauer, 2008; this work). Digits of the dactyloids and skinks surveyed show no expansion of any of their metacarpal or phalangeal extremes, and they also lack of paraphalangeal elements. These combined features might have originated exclusively within Gekkota, and their presence in the fossil hand may be indicative of its gekkotan affinities. Although paraphalanges have been only reported in some gekkotans, they are not diagnostic for higher level groups such as family, and above. Also, many padbearing gekkotans lack of paraphalangeal elements (e.g. Luperosaurus sp., Paragehyra sp. and Phelsuma sp. [Gamble et al., 2012]) and at least one pad-less gecko develops paraphalangeal elements (Homonota sp., this work). It appears that these structures are not a critical component of the gekkotan adhesive or climbing mechanisms.

The fossil hand exhibits twelve small, bean-shaped discoidal structures that we interpret as putative paraphalanges. Although some of them occur as unpaired elements, they might have been arranged in pairs in the living organism (See Fig. 3A). The paired

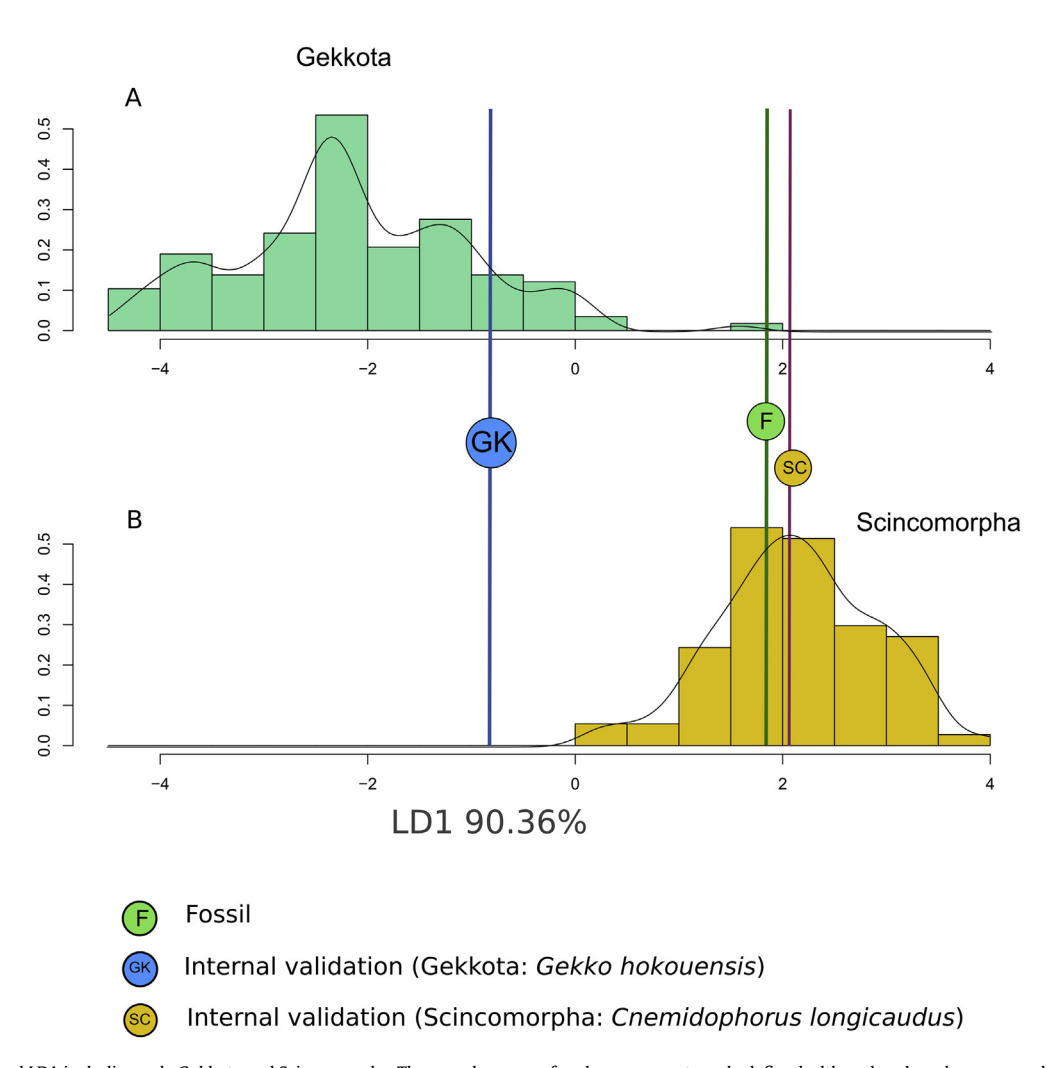


Fig. 5. One-dimensional LDA including only Gekkota and Scincomorpha. The morphozones of each group are strongly defined, although a shared area around 0 is evident. The green vertical line corresponds to the position of the fossil hand, which intersects the central portion of the scincomorph morphozone, and the margin of the gekkotan morphozone.

Table 4Scores of the Linear Discriminant function, representing the position of the specimens in the morphospace. As a result of an analysis based on only two categories (Scincomorpha and Gekkota), a single linear component function (LD1) was obtained. The specimens are ordered by increasing score. Only those specimens with the closest scores to the fossil hand are shown.

Species	Group	Collection number	Ordered scores along LD1
Ameiva ameiva	Scincomorpha	UNNEC 01390	1.23
Emoia adspersa	Scincomorpha	USNM 322732	1.23
Cnemidophorus longicaudus	Scincomorpha	VA. 002/4	1.57
Ameiva ameiva	Scincomorpha	UNNEC 01374	1.61
Cf. Mabuya bicolor	Scincomorpha	UIS R 316	1.65
Ameiva ameiva	Scincomorpha	UNNEC 01391	1.73
Ameiva ameiva	Scincomorpha	ICN 4753	1.74
Mochlus sundevallii	Scincomorpha	MCN 4692	1.78
Marmorosphax tricolor	Scincomorpha	USNM 267844	1.79
Fossil hand	Stem Gekkota	MCZ R-190835	1.84
Mabuya mabouya	Scincomorpha	VA. 002/2	1.92
Emoia longicauda	Scincomorpha	USNM 336680	2.01
Mabuya sp.	Scincomorpha	UIS R 0264	2.01

discoidal structures situated medially and laterally to the distal extremes of the first phalanx of the fourth digit could represent the natural arrangement since they resemble the paraphalangeal elements of some extant pad bearing gekkonids and phyllodactylids (Fig. 3A, Table 2). The putative paraphalanges are also associated with an interphalangeal joint, and are positioned adjacent to the distal phalangeal extremes, as in previously described paraphalanges. It should be noted that in certain cases paraphalanges can be unpaired elements (see fig. 3 in Russell and Bauer, 1988), and can be located in the metacarpophalangeal joint (see figs. 3 and 15 in Russell and Bauer, 1988; Fig. 3A in this work).

There is a wide variety of paraphalangeal morphologies, from small discoidal structures to elongated or wing-like arrangements, including more complex planar structures (Table 1). Gamble et al. (2012) estimated that paraphalanges evolved independently nine times in Gekkonidae and Phyllodactylidae, and that their morphology is largely different in each acquisition event. The paired elements described as putative paraphalanges resemble the paraphalanges of Hemidactylus sp. (Wellborn, 1933; Stephenson, 1960; Fig. 3C this work), Lygodactylus sp., Calodactylodes sp. and Homonota sp. (Russell and Bauer, 1988; Gamble et al., 2012; this work; Fig 2B, Table 1). Their position is very similar to Hemidactylus sp., since they are located at the interphalangeal joint between the first and second phalanges of the fourth digit. There is no evidence regarding their tissue composition; nevertheless, within extant Gekkonidae and Phyllodactylidae, paraphalanges can be cartilaginous, calcified or even ossified structures (Wellborn, 1933; Haacke, 1976: Russell and Bauer, 1988: Gamble et al., 2012: Otero and Hoyos, 2013). In future specimens, the taphonomic properties of the amber faunas might help preserve more details from the other associated tissue types (Poinar and Hess, 1982; Grimaldi et al., 1994; Poinar et al., 1996).

Paraphalangeal elements are proposed to participate in the support of the digital scansors or interdigital webbing (Romer, 1956; Russell, 1975, 2002; Russell and Bauer, 1988), or that help controlling the adhesive subdigital pads when the penultimate phalanx cannot impart appropriate pressure on the scansors. This is consistent with the preserved toepad impressions in amber associated with the fossilized hand MCZ R—190835. Paraphalangeal elements seem to be associated with a variety of biological processes, from climbing and digging, to the grasping function of the limbs (Russell and Bauer, 1988; Higham, 2015; Rothier et al., 2017). The presence of paraphalanges in the padless *Homonota fasciata*

extends the domain of these structures to terrestrial and rupiculous pad-less forms. Although a pad-less condition is considered as the ancestral state of Gekkota, in Phyllodactylidae toepads are widespread, and are lost in *Homonota* and *Garthia* (Gamble et al., 2012). In this group, it can be interpreted that paraphalanges of *Homonota* are vestigial structures once associated with the adhesive pads of their phyllodactylid ancestor.

The discoidal structures seen in the gecko hand can also be interpreted as sesamoids. In extant squamates, there at least two types of sesamoids associated to rays (i.e. the metacarpals and their following phalanges): the sesamoidea digitorum manus and the sesamoidea metacarpale. The sesamoidea digitorum manus (Otero and Hoyos, 2013) are small, unpaired circular and plane structures located in the dorsal side of the terminal joint of digits I to V. These structures are present in several squamate families (e.g. Agamidae, Liolaemidae and Dactyloidae). The sesamoidea metacarpale situated ventro-distally to metacarpals I to V, are dorsoventrally flattened, irregular and of different sizes (see Jerez et al., 2010, their fig. 1C). Within squamates, the sesamoidea metacarpale are seen less frequently than the sesamoidea digitorum manus. Although all these sesamoid types are much more frequent within squamates than the paraphalangeal elements, none of them are situated in the interphalangeal joint as in the fossil hand (Fig. 3A). Moreover, although in taxa bearing both types of digital sesamoids the maximal number of elements is ten, we found at least twelve elements (see Fig. 3A). Other traits from the fossil hand that suggest that those structures are not sesamoids include their similar shape and size, contrary to the usual irregular sesamoid shape (Jerez et al., 2010). Interestingly, paraphalanges have been considered as another type of sesamoids by Kluge (1968) and Otero and Hoyos (2013). Thus, it is possible that paraphalanges are actually one type of sesamoids.

Scansoriality was proposed for the Jurassic stem-gekkotan *Eichstaettisaurus schroederi* and for *Ardeosaurus digitatellus* (Simões et al., 2016) based on a set of climbing adaptations of the cranium and post-cranium. The authors interpreted the elongated penultimate phalanges, in comparison to the intermediate ones, as indicative of climbing habits. Fröbisch and Reisz (2009) also considered this pattern, also present in the fossil hand MCZ R–190835, as an indicator of climbing. Supporting this idea, Rothier et al. (2017) differentiated non-climbing from climbing geckos by their relatively longer ultimate and penultimate phalanges of digit V of the hand.

Although lizards aptitude to climb is reported to have emerged in the Jurassic period (Simões et al., 2016), evidence of scansoriality assisted by a sub-digital adhesive system is observed in the mid-Cretaceous in gekkotans, as revealed by the foot of Cretaceogekko burmae (Arnold and Poinar, 2008) and the fossil hand here described. The pads of MCZ R-190835 (Daza et al., 2016) also show specialized sub-digital structures, indicating that in the middle Cretaceous a certain type of adhesive system was already present on hands and feet. In line with this new interpretation of MCZ R-190835, we identify morphological features that could be applied to the isolated fossil record of Gekkota (Daza et al., 2014) that provide initial insights into the understanding of the evolutionary pathway that originated the sub-digital adhesive system. It should be considered that if these morphological features constitute a specialized anatomical system associated to the sub-digital structures, the improvement of performance might have been considerable. Indeed, it has already been shown that slight modifications in the morphology of those structures can result in dramatic changes in function (Higham et al., 2017).

The brief survey of the morphological diversity displayed by the ungual phalanx presented here shows that some particular

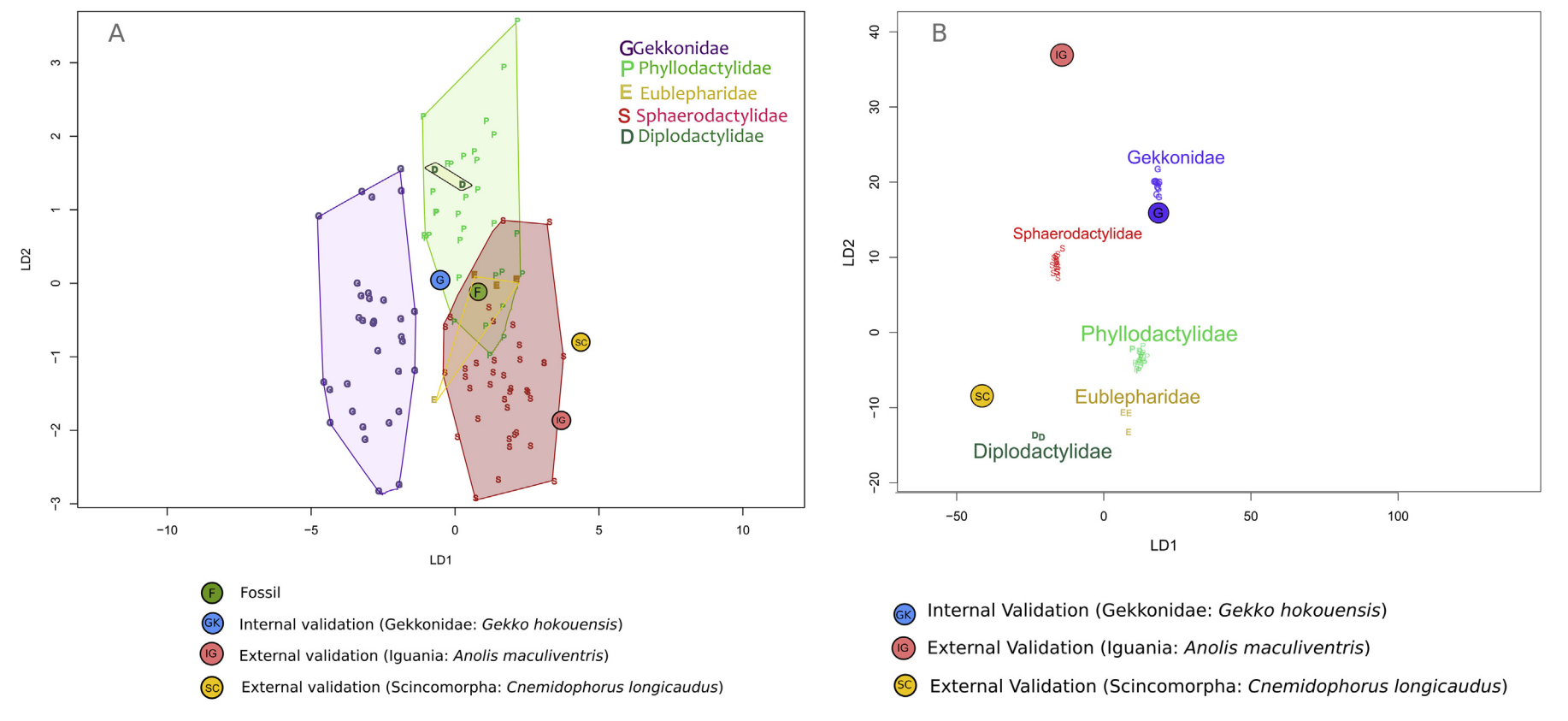


Fig. 6. Two-dimensional LDA analysis of the gekkotan data set based on metacarpal and digital variables. (A) The classification criterion was family membership within the Gekkota. The polygons enclose specimens of each family considered. The morphozones of each group overlap slightly. The fossil plots in the area occupied by the Phyllodactylidae and Eublepharidae. (B) Graphical representation of an LDA constructed using the data set of gekkotan hand measurements. Note that in this figure the fossil hand is not included because we could not measure its carpal bones.

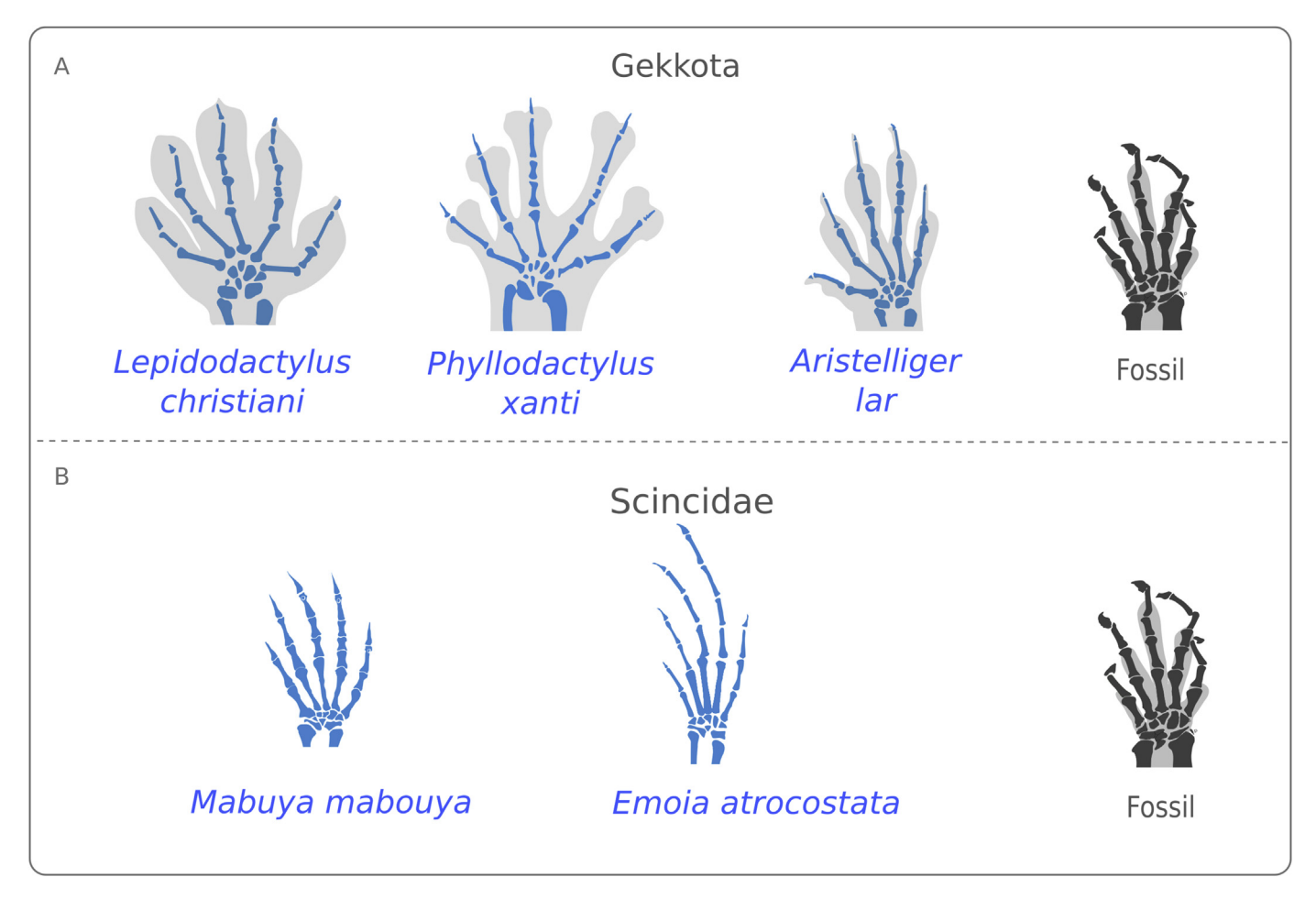


Fig. 7. Schematic diagrams showing the relationship between the pad surface and the bones of the manus in pad-bearing geckos. (A) The length of the metacarpal bones is subequal in *Lepidodactylus christiani*. The fifth metacarpal of *Phyllodactylus xanti* is longer than the first. In *Aristelliger lar* the first and fifth metacarpals are subequal in length and these are shorter than the second, third and fourth metacarpals, which are themselves subequal in length. In all these hands, the distal extreme of some phalanges and metacarpal are greatly expanded. The fossil hand is included in order to facilitate comparisons. (B) Schematic diagrams showing the skeletal configuration of the manus of some scincids. In *Mabuya* sp. the first and fifth metacarpals are subequal in length and these are shorter than the second, third and fourth metacarpals, which are themselves subequal in length. *Emoia* sp. has its first and fifth metacarpals of subequal length and these are the shortest. The second is the next longest, and the third and fourth are subequal and the longest. The fossil hand is included for comparison.

features, such as the presence of an acute downward inflection and dorsal concavity observed in the fossil hand MCZ R-190935, occur in a wide diversity of lizards. It has been shown that ungual and claw morphology is mostly shaped by ecological factors, and is strongly associated with locomotion modes (Feduccia, 1993; Hamrick, 1998; Zani, 2000; Tulli et al., 2009; Tulli et al., 2016; Tinius and Russell, 2017). The fossil hand morphotype is also found in the claws of climbing species, such as Iguana iguana, Urostrophus gallardoi, Pristidactylus valeriae, Anisolepis longicaudus, Liolaemus chilensis, and arboreal Anolis lizards. Such ungual phalanges are relatively tall at their base (Table 2) and their morphology has been associated with the exploitation of vertical habitats (both arboreal and rupiculous) (Zani, 2000; Tulli et al., 2009; Simões et al., 2016). The presence of this morphology in the fossil hand suggests that it comes from a scansorial lizard. The tall base of the ungual phalanx, plus the sharp downward inflection, are associated with the mechanically advantageous action of the flexor tendon of the digit, which provides a greater lever arm, thus increasing the effectiveness of penetrating and grasping the substrate (Russell, 1975; Simões et al., 2016).

When considering the divergence angle between the first and fifth metacarpals (52° in the fossil hand) we are aware that this

measurement is susceptible of being affected by preservation issues. It has been reported that pad-bearing lizards generally arrange their digits in a broad arc (Russell et al., 1997; Fontanarrosa and Abdala, 2014; Fontanarrosa and Abdala, 2016). The diverging arrangement of the digits of pad-bearing geckos could contribute to the contact of the adhesive system with vertical surfaces, regardless of the orientation of the body (Russell et al., 1997). Nevertheless, within gekkotans, the digital angles vary from around 43° (e.g. Pseudogonatodes guianensis) to 196° (e.g. Tarentola annularis) (GF pers. obs.). Thus, the fossil hand exhibits a narrow angle that fits in the reported range of the Gekkota.

Considering the dataset that includes data from Scincomorpha, Iguania and Gekkota, the location of the fossil specimen within the combined morphospace fell within the Scincomorpha morphozone (Fig. 4A). Such a classification must be interpreted with caution given that data of the fossil hand places it close to members of all three main categories examined in the analysis: Iguania, Scincomorpha and Gekkota. Indeed, specimens plotted closest to the fossil hand belong to Scincomorpha (e.g., Ameiva ameiva), Iguania (e.g., Polychrus acutirostris) and Gekkota (e.g., Pseudogonatodes peruvianus) (Table 3). The fossil hand is located in a region not too far from the edge of the morphospace circumscribing the

Scincomorpha. This inability of the LDA to effectively separate the specimens by taxonomic membership can be due to the fact that our data set does not take into account the enormous number of species within all three groups, and might thus not reflect the entire shape envelope of any of them. Considering Scincomorpha and Gekkota only, the common region of the morphospace occupied by both taxa is more evident. This pattern represents the convergence of some Gekkota nested within the morphospace of Scincomorpha. Intriguingly, the opposite situation occurs with certain extant Scincidae (Lipinia sp. and Prasinohaema sp.) that are convergently nested within Gekkota because of their adhesive pads (Irschick et al., 1996). Alternatively, the osteology of the hand of MCZ R-190835 could represent the plesiomorphic condition, reflecting an early stage in the evolution of manual proportions of climbing forms. This possibility is supported by the biometric affinity of MCZ R-190835 with *Polychrus acutirostris*, a padless climber. Interestingly, Sukhanov (1961) already proposed that Scincomorpha and Gekkota share plesiomorphic characters in relation to the locomotor musculature, thus supporting the pervasive affinities of these taxa and the existence of the Scincogekkonomorpha clade (Conrad, 2008; Bolet and Evans, 2012).

The third analytical step, in which we considered data exclusive of Gekkota, for which the carpal region variables were not taken into account, failed to reveal a clear separation between groups of specimens by family. The fossil is projected into the area occupied by Phyllodactylidae and Eublepharidae (Fig. 6A). Taking all sources of evidence into account, we propose that MCZ R—190835 is a hand of a gekkotan lizard. Thus, we interpret the biometric affinities as further supporting the already reported highly frequent convergent phenomena between geckos and scincids (Irschick et al., 1996; Pianka and Vitt, 2003).

5. Conclusions

The taxonomic allocation of the fossil hand MCZ R-190835 varies according to the evidence used. The results from the morphological and morphometric analyses indicate that the fossil hand is either a scincomorph or a gekkotan. The morphometric data indicates that the gecko hand is more similar to Scincoidea than to Gekkota or Iguania. The morphospace area occupied by the fossil hand is also shared with other lizard groups (e.g. agamids, teiids, and gekkotans). This position of the gecko hand in the morphospace is ambiguous and might be reflecting the existent morphometric similarities of the hand anatomy in members of Gekkota and Scincomorpha. The morphological evidence is more conclusive and the shape of skeletal elements support Gekkotan affinities. The presence of putative paraphalangeal elements in MCZ R-190825 represents the first report of these structures in any fossil, and documents the presence of sophisticated digital structures in a 99 Ma lizard. These structures, together with the presence of expanded distal extremes in some phalanges, followed by a slender phalanx in the fossil hand, are a combination of features that co-occur within certain pad-bearing species of extant geckos such as Thecadactylus sp. and Gehyra mutilata. The absence of expansion in any of the metacarpal or phalangeal distal ends in other pad-bearing lizards (e.g. Dactyloa and Prasinohaema) reinforce the allocation of this fossil to Gekkota. Our analyses failed to predict its position within the extant Gekkota families surveyed, consistently with ongoing analyses of Cretaceous geckos that form the sister clade of Gekkota (Stem-Gekkota). The fine structures preserved in the fossil hand provides certain clues about the early origin of scansoriality in gekkotan by means of a sophisticated adhesion system. Finally, paraphalanges are present in both pad bearing and padless gekkotans, indicating that these accessory structures of the toe-pad are not a necessary component of the adhesive mechanism of gekkotans.

Acknowledgments

We wish to recognize the helpful discussions and comments by Aaron M. Bauer, who critically read the current manuscript. We are also deeply indebted to the Comparative Zoology Museum of Harvard, and its director lames Hanken, for purchasing the specimen. We are grateful to the Editor-in-Chief of Cretaceous Research. Eduardo Koutsoukos, who helped us in several aspects. We would like to deeply thank the detailed reviews of Anthony Russell and David Marjanović, who generously dedicated much of their time to improve this manuscript. Olivia Clark (Sam Houston State University) provided several comments that improved the quality of this manuscript. We are also grateful to María José Tulli, Cristian Abdala, Marcos Paz, Marta Cánepa, Sonia Kretzschmar and Gustavo Schrocchi (UEL, CONICET-FML), Fernando Lobo (IBIGEO, CONICET), Felix Cruz (INIBIOMA, CONICET-UNCOMA), Martha Patricia Ramirez (Universidad Industrial de Santander, Colombia), Julio Mario Hoyos (Universidad Javeriana, Colombia) for their generous help in obtaining many of the lizard specimens.

References

- Augé, M., 2005. Évolution des lézards du Paléogène en Europe. Mémoires du Muséum national d'Historie naturelle 192, 1—369.
- Arnold, E.N., Poinar, G., 2008. A 100 million year old gecko with sophisticated adhesive toepads preserved in amber from Myanmar. Zootaxa 1847, 62–68.
- Bolet, A., Evans, S.E., 2012. A tiny lizard (Lepidosauria, Squamata) from the Lower Cretaceous of Spain. Palaeontology 55, 491–500.
- Cartmill, M., 1985. Climbing. In: Hildebrand, M., Bramble, D.M., Liem, K.F., Wake, D.B. (Eds.), Functional Vertebrate Morphology. Belknap Press, Cambridge, pp. 73–88.
- Conrad, J.L., 2008. Phylogeny and systematics of Squamata (Reptilia) based on morphology. Bulletin of the American Museum of Natural History 310, 1—182.
- Daza, J.D., Bauer, A.M., Snively, E.D., 2014. On the fossil record of the Gekkota. Anatomical Record 297, 433–462.
- Daza, J.D., Stanley, E.L., Wagner, P., Bauer, A.M., Grimaldi, D.A., 2016. Mid-Cretaceous amber fossils illuminate the past diversity of tropical lizards. Science Advances 2, e1501080.
- Estes, R., 1983. The fossil record and the early distribution of lizards. In: Rhodin, A.G.J., Miyata, K. (Eds.), Advances in Herpetology and Evolutionary Biology: Essays in Honor of E. E. Williams. Museum of Comparative Zoology, Cambridge, pp. 365–398.
- Estes, R., de Queiroz, K., Gauthier, J., 1988. Phylogenetic relationship within Squamata. In: Estes, R., Pregill, G. (Eds.), Phylogenetic Relationships of the Lizard Families. Stanford University Press, Stanford, pp. 119—281.
- Feduccia, A., 1993. Evidence from claw geometry indicating arboreal habits of *Archaeopteryx*. Science 259, 790–793.
- Fontanarrosa, G., Abdala, V., 2014. Anatomical analysis of the lizard carpal bones in the terms of skilled manual abilities. Acta Zoologica 95, 249–263.
- Fontanarrosa, G., Abdala, V., 2016. Bone indicators of grasping hands in lizards. PeerJ 4. e1978.
- Fröbisch, Jörg, Reisz, Robert R., 2009. The Late Permian herbivore Suminia and the early evolution of arboreality in terrestrial vertebrate ecosystems. Proceedings. Biological Sciences/The Royal Society 276 (1673), 3611–3618.
- Gamble, T., Greenbaum, E., Jackman, T.R., Russell, A.P., Bauer, A.M., 2012. Repeated origin and loss of adhesive toepads in geckos. PLoS One 7, e39429.
- Gauthier, J.A., Kearney, M., Maisano, J.A., Rieppel, O., Behlke, A.D.B., 2012. Assembling the squamate tree of life: perspectives from the phenotype and the fossil record. Bulletin of the Peabody Museum of Natural History 53, 3–308.
- Grimaldi, D.A., 1996. Amber: Window to the Past. American Museum of Natural History, New York 216.
- Grimaldi, D.A., Bonwich, E., Delannoy, M., Doberstein, S., 1994. Electron microscopic studies of mummified tissues in amber fossils. American Museum Novitates 3097. 1–31.
- Haacke, W.D., 1976. The burrowing geckos of southern Africa, 5 (Reptilia: Gekkonidae). Annals Transvaal Museum 30, 71–89.
- Hamrick, M.W., 1998. Functional and adaptive significance of primate pads and claws: evidence from New World anthropoids. American Journal of Physical Anthropology 106, 113–127.
- Higham, T.E., 2015. Bolting, bouldering, and burrowing: functional morphology and biomechanics of pedal specialisations in desert-dwelling lizards. In: Bininda-Emonds, O.R.P., Powell, G.L., Jamniczky, H.A., Bauer, A.M., Theodor, J. (Eds.), All Animals are Interesting: a Festschrift in Honour of Anthony P. Russell. BIS-Verlag der Carl von Ossietzky Universität Oldenburg, Oldenburg, pp. 279–301.
- Higham, T.E., Birn-Jeffery, A.V., Collins, C.E., Hulsey, C.D., Russell, A.P., 2015. Adaptive simplification and the evolution of gecko locomotion: morphological and biomechanical consequences of losing adhesion. Proceedings of the National Academy of Sciences 112, 809–914.

- Higham, T.E., Gamble, T., Russell, A.P., 2017. On the origin of frictional adhesion in geckos: small morphological changes lead to a major biomechanical transition in the genus *Gonatodes*. Biological Journal of the Linnean Society 120, 503—517.
- Irschick, D.J., Austin, C.C., Petren, K., Fisher, R.N., Losos, J.B., Ellers, O., 1996. A comparative analysis of clinging ability among pad-bearing lizards. Biological Journal of the Linnean Society 59, 21–35.
- Izadi, H., Stewart, K.M.E., Penlidis, A., 2014. Role of contact electrification and electrostatic interactions in gecko adhesion. Journal of the Royal Society Interface 11, 2014371.
- Jerez, A., Mangione, S., Abdala, V., 2010. Occurrence and distribution of sesamoid bones in squamates: a comparative approach. Acta Zoologica (Stockholm) 91, 295–305.
- Kluge, A.G., 1968. Phylogenetic relationships of the gekkonid lizard genera *Lepidodactylus* Fitzinger, *Hemiphyllodactylus* Bleeker, and *Pseudogekko* Taylor. Philippine Journal of Science 95, 331–352.
- Kümmell, S.B., Frey, E., 2012. Digital arcade in the autopodia of Synapsida: standard position of the digits and dorsoventral excursion angle of digital joints in the rays II—V. Palaeobiodiversity and Palaeoenvironments 92, 171—196.
- Neumann, D.A., 2010. Kinesiology of the Musculoskeletal System: Foundations for Physical Rehabilitation, second ed. Mosby, Maryland Heights. 725 p.
- Otero, T., Hoyos, J.M., 2013. Sesamoid elements in lizards. Herpetological Journal 23, 105–114.
- Pianka, E.R., Vitt, L.J., 2003. Lizards: Windows to the Evolution of Diversity. University of California Press, Berkeley, 333 p.
- Poinar, G.O., Hess, R., 1982. Ultrastructure of 40 million year old insect tissue. Science 215, 1241–1242.
- Poinar, H.N., Hoss, M., Bada, J.L., Paäbo, S., 1996. Aminoacid racemization and the preservation of ancient DNA. Science 272, 864–866.
- R Development Core Team, 2011. R: a Language and Environment for Statistical Computing, Reference Index Version 2.2.1. R Foundation for Statistical Computing, Vienna. http://www.R-project.org.
- Romer, A.S., 1956. The Osteology of the Reptiles. University Chicago Press, Chicago, 772 p.
- Ross, A., 2010. Amber: the Natural Time Capsule. Natural History Museum, London, 112 p.
- Rothier, P.S., Brandt, R., Kohlsdorf, T., 2017. Ecological associations of autopodial osteology in Neotropical geckos. Journal of Morphology 278, 290–299.
- Rubidge, B.S., 2013. The roots of early mammals lie in the Karoo: Robert Broom's foundation and subsequent research progress. Transactions of the Royal Society of South Africa 68, 41–52.
- Russell, A.P., 1975. A contribution to the functional analysis of the foot of the Tokay, *Gekko gecko* (Reptilia: Gekkonidae). Journal of Zoology London 176, 437–476.
- Russell, A.P., 2002. Integrative functional morphology of the gekkotan adhesive system (Reptilia: Gekkota). Integrative and Comparative Biology 42, 1154–1163.
- Russell, A.P., Bauer, A.M., 1988. Paraphalangeal elements of gekkonid lizards: a comparative survey. Journal of Morphology 197, 221–240.

- Russell, A.P., Bauer, A.M., 2008. The appendicular locomotor apparatus of Sphenodon and normal-limbed squamates. In: Gans, C., Gaunt, A.S., Adler, K. (Eds.), Biology of Reptilia, Volume 21, Morphology I. The Skull and Appendicular Locomotor Apparatus of Lepidosauria. Society for the Study of Reptiles and Amphibians, Ithaca, pp. 1–465.
- Russell, A.P., Bauer, A.M., Laroiya, R., 1997. Morphological correlates of the secondarily symmetrical pes of gekkotan lizards. Journal of Zoology 241, 767–790.
- Schindelin, J., Arganda-Carreras, I., Frise, E., Kaynig, V., Lonair, M., Pietzch, T., Preibisch, S., Rueden, C., Saalfeld, S., Schmid, B., Tinevez, J.Y., White, D.J., Hartenstein, V., Eliceiri, K., Tomancak, P., Cardona, A., 2012. Fiji: An open-source platform for biological-image analysis. Nature Methods 9, 676–682.
- Shi, G., Grimaldi, D.A., Harlow, G.E., Wang, J., Wang, J., Yang, M., Lei, W., Li, Q., Li, X., 2012. Age constraint on Burmese amber based on U–Pb dating of zircons. Cretaceous Research 37. 155–163.
- Simões, T.R., Caldwell, M.W., Nydam, R.L., Jiménez-Huidobro, P., 2016. Osteology, phylogeny, and functional morphology of two Jurassic lizard species and the early evolution of scansoriality in geckoes. Zoological Journal of the Linnean Society 180, 216–241.
- Stephenson, N.G., 1960. The comparative osteology of Australian geckos and its bearing on their morphological status. Zoological Journal of the Linnean Society 44, 278–299.
- Sukhanov, V.B., 1961. Some problems of the phylogeny and systematics of Lacertilia (seu Sauria). Zoologischeskiy Zhurnal 40, 73–83.
- Tinius, A., Patrick Russell, A., 2017. Points on the curve: An analysis of methods for assessing the shape of vertebrate claws. Journal of Morphology 278, 11–286.
- Tulli, M.J., Cruz, F.B., Herrel, A., Vanhooydonck, B., Abdala, V., 2009. The interplay between claw morphology and microhabitat use in iguanian lizards. Zoology 112, 379–392.
- Tulli, M.J., Carrizo, L.V., Samuels, J.X., 2016. Morphological variation of the forelimb and claw in Neotropical sigmodontine rodents (Rodentia: Cricetidae). Journal of Mammalian Evolution 23, 81–91.
- Uetz, P., Freed, P., Hošek, J., 2017. The Reptile Database. http://www.reptile-database.org. (Accessed 12 September 2017).
- Wassersurg, R.J., 1976. A procedure for differential staining of cartilage and bone in whole formalin-fixed vertebrates. Stain Technology 51, 131–134.
- Wellborn, V., 1933. Vergleichede osteologishe Untersuchungen an Geckoniden, Eublephariden und Uroplatiden. Sitzungsberichte der Gesellschaft Naturforschender Freunde zu Berlin 1933, pp. 126–199.
- Zani, P.A., 2000. The comparative evolution of lizard claw and toe morphology and clinging performance. Journal of Evolutionary Biology 13, 316–325.

Appendix A. Supplementary data

Supplementary data related to this article can be found at https://doi.org/10.1016/j.cretres.2017.11.003.